BNL-66691

JOURNAL OF GEOPHYSICAL RESEARCH, VOL. 105, NO. D1, PAGES 1367–1385, JANUARY 20, 2000

A description of the global sulfur cycle and its controlling processes in the National Center for Atmospheric Research Community Climate Model, Version 3

Philip J. Rasch, Mary C. Barth, and Jeffrey T. Kiehl

National Center for Atmospheric Research, Boulder, Colorado

Stephen E. Schwartz and Carmen M. Benkovitz

Brookhaven National Laboratory, Upton, New York

Abstract. We examine the balance between processes that contribute to the global and regional distributions of sulfate aerosol in the Earth's atmosphere using a set of simulations from the National Center for Atmospheric Research Community Climate Model, Version 3. The analysis suggests that the seasonal cycle of SO_2 and SO_4^{2-} are controlled by a complex interplay between transport, chemistry and deposition processes. The seasonal cycle of these species is not strongly controlled by temporal variations in emissions but by seasonal variations in volume of air processed by clouds, mass of liquid water serving as a site for aqueous chemistry, amount of oxidant available for the conversion from SO_2 to SO_4^{2-}, vertical transport processes, and deposition. A tagging of the sulfate by emission region (Europe, North America, Asia, and rest of world [ROW]), chemical pathway (gaseous versus in-cloud), and type of emissions (anthropogenic versus biogenic) is used to differentiate the balance of processes controlling the production and loading from this material. Significant differences exist in the destiny of SO_2 molecules emitted from the several regions. An SO_2 molecule emitted from the ROW source region has a much greater potential to form sulfate than one emitted from, for example, Europe. A greater fraction of the SO_2 molecules is oxidized that originate from ROW compared with other areas, and once formed, the sulfate has a longer residence time (that is, it is not readily scavenged). The yield of sulfate from ROW sources of SO_2 is a factor of 4 higher than that of Europe. A substantially higher fraction of the SO_2 emitted over Europe is oxidized to sulfate through the ozone pathway compared to other regions. The analysis suggests that there are significant differences in the vertical distribution, and horizontal extent, of the propagation of sulfate emitted from the several source regions. Sulfate from Asian source regions reaches the farthest from its point of origin and makes a significant contribution to burdens in both hemispheres, primarily from plumes reaching out in the upper troposphere. Sulfate from other source regions tends to remain trapped in their hemisphere of origin.

1. Introduction

Sulfur emissions from industry, and from natural (biogenic and volcanic) sources are believed to influence the earths climate in a number of ways. Emissions of these sulfur bearing compounds can rapidly form aerosol particles that act to modulate directly the earth's radiation budget by absorbing and scattering radiation [*Charlson et al.*, 1992], and to influence indirectly many aspects of climate through their interaction with clouds. By serving as cloud condensation nuclei (CCN) they influence the number and size of cloud droplets, and this has a role in influencing the clouds radiative properties [*Twomey*, 1974], and the lifetime and precipitation properties of clouds [*Albrecht*, 1989]. Concern about the potential climatic effects of the anthropogenic emission of sulfur species into the atmosphere has motivated numerous studies over the last 10 years [e.g., *Langner and Rodhe*, 1991; *Feichter et al.*, 1996; *Chin and Jacob*, 1996; *Feichter et al.*, 1997]. In spite of intense study of the atmosphere's sulfur cycle over the past 20 years there are still large gaps and uncertainties in our knowledge about this important component of the Earth's climate system.

This paper is the second in a sequence of three describing our efforts to improve our knowledge about the sulfur cycle in the atmosphere. *Barth et al.* [this issue] (hereinafter referred to as part 1) describes the basic model used in the studies, compares the model simulation to recent observations

Copyright 2000 by the American Geophysical Union.

Paper number 1999JD900777.
0148-0227/00/1999JD900777$09.00

of sulfur species, and discusses ways in which the aqueous photochemistry influenced the model sulfur cycle.

Here (part 2) we adopt a broader view, and describe our model's picture of the life cycle of sulfur in terms of all the processes that control the dominant sulfur species of the atmosphere. Our primary focus is to follow the sulfur atoms as they are emitted (primarily as biogenic dimethyl sulfide (DMS) or anthropogenic SO_2) through chemical transformation, transport, and deposition processes, with the goal of identifying the processes that control sulfate aerosol regionally and seasonally. These controlling processes are revealed by "tagging" of components of the sulfur cycle in a manner similar to *Benkovitz et al.* [1994], although their focus was on the North Atlantic region over a 2 month time span. *Kiehl et al.* [1999] (hereinafter referred to as part 3) use the model described by parts 1 and 2 to discuss the predicted direct and indirect radiative forcing by aerosols and the potential for the anthropogenic component to affect climate.

2. Model Description

Several previous studies of the global sulfur budget have been performed in the context of "off-line transport models" [*Langner and Rodhe*, 1991; *Chin et al.*, 1996; *Chuang et al.*, 1997; *Pham et al.*, 1995; *Kasibhatla et al.*, 1997]. The sulfur cycle in the present study evolves within a general circulation model framework. There is significantly more temporal and physical detail available about many processes that influence aerosol formation and their interaction with clouds, climate, and chemistry in a general circulation model (GCM) compared to an off-line model. In constrast to off-line models where the meteorology is specified by interpolating between snapshots spaced 3-6 hours (or even longer) apart GCM solutions are advanced with meteorological information evolving over short (order 20 minute) timesteps. Complete three-dimensional distributions of cloud volumes, condensate amounts, and rate of conversion to precipitation, etc. are available in GCMs. Most off-line models must approximately reconstruct this information from two-dimensional (surface) distributions. The three-dimensional fields provide an increased level of consistency with other meteorological information that is difficult to achieve in the off-line models. Our GCM configuration is quite similar to that described by *Feichter et al.* [1996, 1997] or *Graf et al.* [1997] in the European Center/Hamburg ECHAM4 model. A GCM predicting sulfate that also includes an elaborate representation of the photochemistry of the troposphere was described by *Lelieveld et al.* [1997] and *Roelofs et al.* [1998].

Details of the model are provided in part 1, but here we repeat a few relevant points. This model is comprised of the basic National Center for Atmospheric Research Community Climate Model (CCM3), [*Kiehl et al.*, 1996], augmented with a prognostic cloud water scheme [*Rasch and Kristjánsson*, 1998], and the photochemistry, scavenging, and deposition processes described by part 1.

The model is run at the nominal NCAR CCM3 horizontal resolution of 2.8 x 2.8 degrees, and a variable vertical resolution, with 18 models layers extending from the surface to ~35 km. A centered time step of 20 min is used for the CCM3 model dynamics, and a consistent approach for cloud and chemistry calculations requires that the transport and most of the chemical processing are advanced from time level $n-1$ to $n+1$ (a 40-min time step). This numerical technique can result in a decoupling of solutions at even and odd time steps. Therefore a time filter [*Asselin*, 1972] is employed to couple the even and odd time step simulations. The aqueous chemistry is integrated independently using a 2-min time step to treat the strong sensitivity of the S(IV) + O_3 reaction rates to the time-dependent pH evolution. Oxidant distributions and the H_2O_2 precursor HO_2 in the present model are prescribed from an independent run of the off-line transport model Intermediate Model for the Annual Global Evolution of Species (IMAGES) [*Müller and Brasseur*, 1995]. The evolution of 4 chemical species are calculated by the model, DMS, SO_2, SO_4^{2-}, and H_2O_2. The treatment of H_2O_2 is considered important because of the strong interaction of SO_2 and H_2O_2 in clouds. Most other global models use a "recovery time" (sometimes instantaneous) of H_2O_2 after oxidation and scavenging to a prescribed distribution.

The model represents emissions of DMS and anthropogenic sulfur species (assumed to be 98% SO_2 and 2% SO_4^{2-}) according to the Global Emissions Inventory Activity (GEIA) 1B.1 database following *Benkovitz et al.* [1996]. Notably lacking are representations for volcanic emissions and the photochemistry associated CS_2 and carbonylsulfide (COS).

The sulfate aerosol formed by the model would strongly influence the model climate if it were allowed to interact with other physical processes, but in these runs we have deliberately disconnected the mechanisms through which these climate feedbacks could take place. Sulfate is treated as a passive tracer. As mentioned in the introduction, a series of simulations have been made in which the sulfur has been tagged. The runs are of differing length, but all have identical meteorology for a common time period. A 7 year run was made in which SO_2 and SO_4^{2-} were tagged according to whether they were of anthropogenic or biogenic origin, and their chemical pathway of formation (i.e. whether the sulfate originated as a result of gas phase or aqueous phase oxidation). A 3 year run was also made where the constituents were tagged by the region of origin.

The meteorological processes of the CCM3 are thoroughly described in a special issue of the Journal of Climate (*Randall*, 1998),and *Rasch and Kristjánsson* [1998], which contain comparisons to clouds, precipitation, winds, boundary layer properties and many other meteorological fields to observational estimates. The CCM is generally quite realistic in its climate simulation, but there are biases that can effect the sulfate simulation. Summertime cloud cover is low over continents (see part 3 for some indication of this bias). The amplitude of the seasonal cycle of precipitation over the continental United States is often higher than seen in the observations, and precipitiation over central Europe shows a maximum in spring and a minimum in late fall not seen in the observations which are nearly constant over the

year. Generally, the models biases are not larger than those characteristic of other off-line chemical transport models or other GCMs. Differences like these with observations will contribute to bias in all global sulfer models in use today.

Spatial distributions of column burdens of species and some of the characteristic partitioning by (anthropogenic and biogenic) origin and chemical pathway were shown in part 1. In the following sections we use these tagged properties along with the region of origin tagging to infer a variety of properties of the atmospheric sulfur cycle as represented in the model.

3. Global Properties

The distribution of anthropogenic and biogenic emissions of sulfate precursors vary significantly over the globe. SO_4^{2-} from anthropogenic emissions dominates the sulfate column burden throughout the troposphere. For this study we have partitioned the emissions into 4 regions defined in Table 1. The spatial distribution of anthropogenic emissions is shown in Plate 1. Seasonal variations of anthropogenic and biogenic emissions for these regions are displayed in Figure 1. The European and American source regions are associated primarily with industrial SO_2 production through coal and petroleum use. The Asian source (which also includes most of the eastern part of Russia) is due primarily to coal burning. The rest of world (ROW) source emissions are often associated with metal-smelting operations in the South America and southern Africa region, and with oil processing in middle eastern countries and industry in Australasia. Despite its small geographic area, Europe emits the most SO_2 and has the largest seasonal variation in emission. Emissions from Europe are a factor of 3 higher than those from the ROW region, which has the lowest emission rate despite occupying ~6 times more surface area than Europe. Biogenic DMS emissions are small in all regions except the ROW area where they constitute approximately half the total emissions in that region. The ROW DMS emissions peak in Southern Hemisphere summer.

Figure 2 shows a time series for the 7-year run for SO_2 and SO_4^{2-}. Initial concentrations for these species were set to zero. The atmosphere has been divided up into 4 layers of approximately equal dry air mass (250 hPa), to show the seasonal cycle of these constituents and their secular trend. The very strong seasonal cycle in SO_2 burdens in the lower troposphere, with a maximum in the lower troposphere during winter, is commonly observed in nature and other models as well. There are regional differences in phase and amplitude of this seasonal variation (discussed in more detail later). The peak in SO_4^{2-} burden is out of phase with that of SO_2 by about half a year.

After transients have died out (~3 years), there are still interannual variations in layer mean burdens of 20%. SO_4^{2-} shows a maximum at all levels in late summer. At this time the SO_2 and SO_4^{2-} are present in substantial amounts at altitudes where scavenging of SO_2 is not effective (because in the present model it is scavenged only in the liquid phase) and where scavenging of SO_4^{2-} acts only through below-cloud collection processes. Although the initial transients in the global burden of SO_2 have decayed after the first year, the mass of SO_4^{2-} contained in the upper troposphere and stratosphere continues to increase for the first 3 years. In these regions, timescales of production, mixing, and removal are much longer than in the lower troposphere. This result is consistent with other modeling studies in which equilibration in the upper troposphere and stratosphere has been examined. For example, *Hartley et al.* [1994] required an equilibration time of 1 year in a series of simulations of $CFCl_3$ to calculate the atmospheric lifetime of this constituent, which is photolyzed in the stratosphere. *Waugh et al.* [1997] found transport times both from modeling and observational data of 0.8 years to the tropical tropopause from the surface, and 3-5 years for the signal to reach middle to high latitudes in the lower troposphere. Our SO_4^{2-} burden in the upper troposphere and stratosphere (order 0.15 Tg S in the uppermost layer) is quite high, significantly higher than that of the comparable study of *Graf et al.* [1997] but (as shown by *Barth et al.* [this issue]) consistent with the estimated upper troposphere and stratosphere background values of *Kent et al.* [1994], or the 0.12 Tg S for the stratosphere cited in a review paper of stratospheric aerosols by *Turco et al.* [1982]. The present model is missing much of the relevant photochemistry, and aerosol microphysics for a good representation in this region of the atmosphere, and more precise characterizations of aerosol are required before we can comment more definitively on the upper tropospheric and stratospheric loading. The long time for equilibration in the upper troposphere/stratosphere suggests caution is needed in assessing the upper troposphere and/or stratospheric loadings in runs made over a relatively short period of time [e.g., *Langner and Rodhe*, 1991; *Benkovitz et al.*, 1994; *Chin et al.*, 1996; *Wojcik and Chang*, 1997]. If our upper tropospheric burdens of sulfate calculated in this model are indeed too high, other mechanisms for its removal must be investigated (e.g., through scavenging of SO_2 on ice or aerosol coagulation and settling).

Table 1. Definition of Regions Used in This Study

Region	Abbreviation	Latitude Range	Longitude Range	Percent of Earth's Surface
North America	NA	15°-90°N	170°E-45°W	13
Europe	Eu	21°-90°N	43°W-64°E	10
Asia	As	0°-90°N	68°-170°E	17
Rest of world	ROW	everthing	else	60

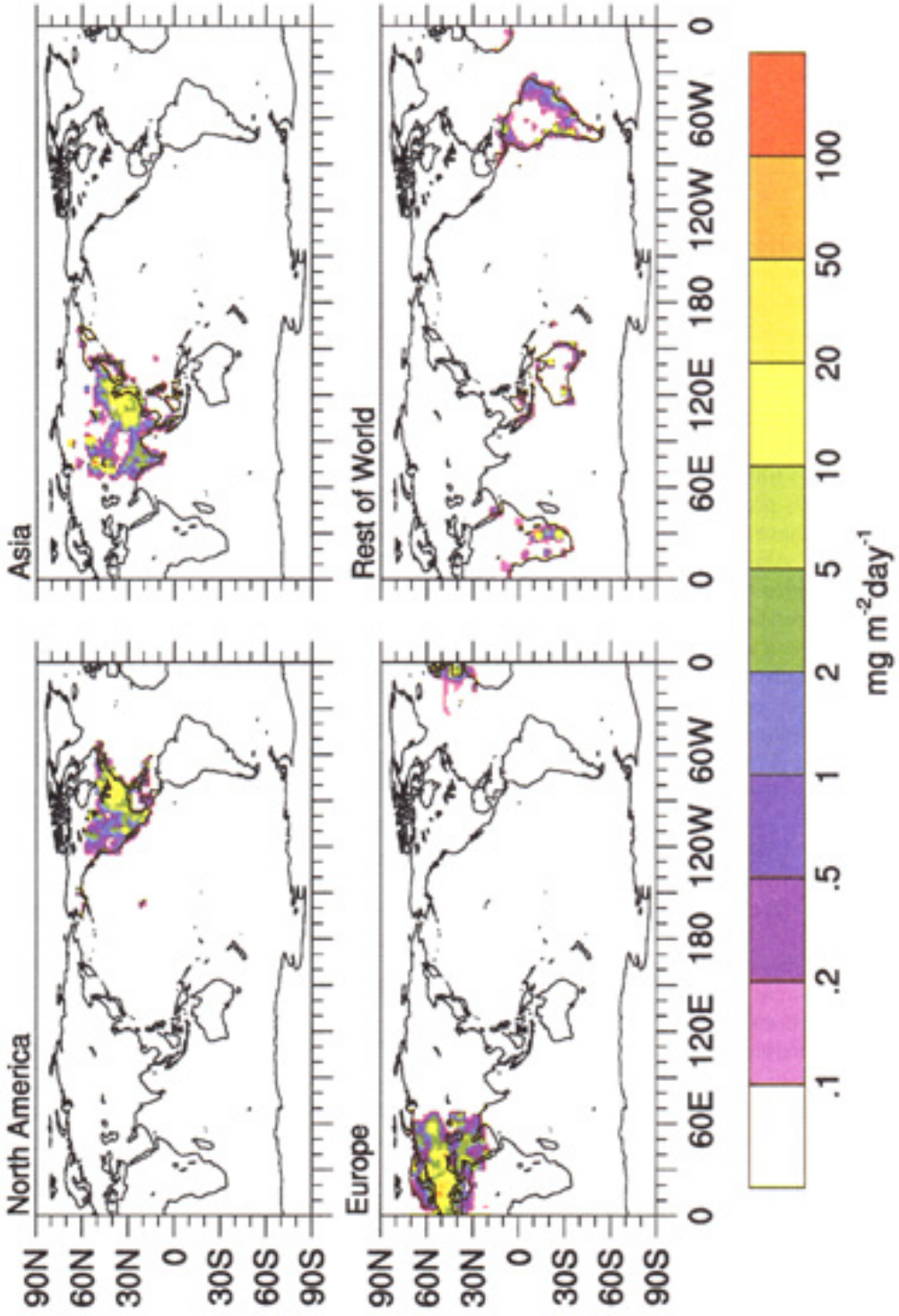

Plate 1. The geographic distribution of annually averaged anthropogenic SO_2 emissions for each of the tagged regions.

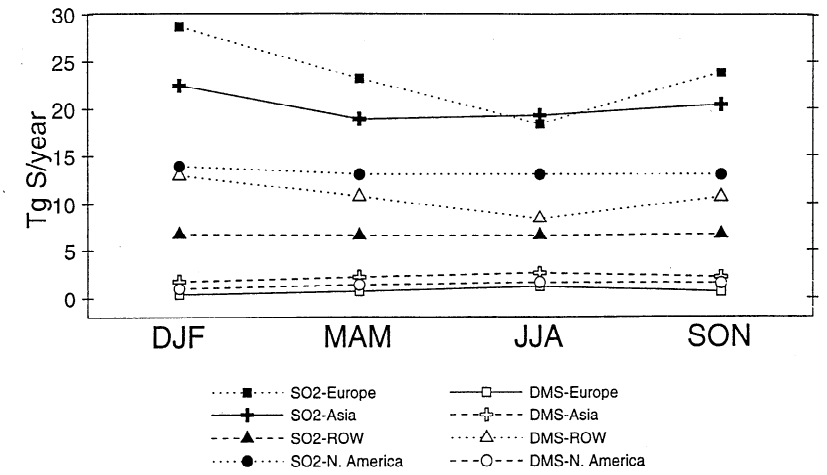

Figure 1. Time series of the seasonal variation in sulfur emissions for the 4 regions utilized in this study. The lines drawn between seasonal means indicate the linear variation used in the interpolated emissions within the model.

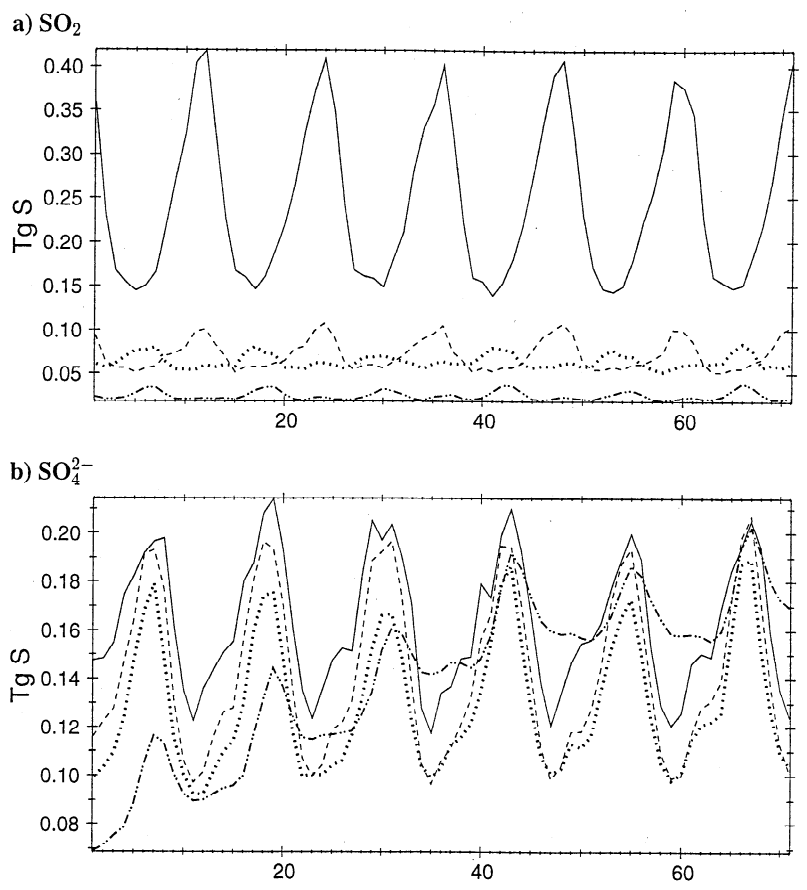

Figure 2. The evolution of the global burden of (a) SO_2 and (b) SO_4^{2-} over the seven year simulation period. The solid line shows the burden in the lowest 250 hPa of the atmosphere. The dashed, dotted, and dash-dotted lines show successively higher 250 hPa layers of the atmosphere respectively. Month 1 corresponds to the first January of the model simulation.

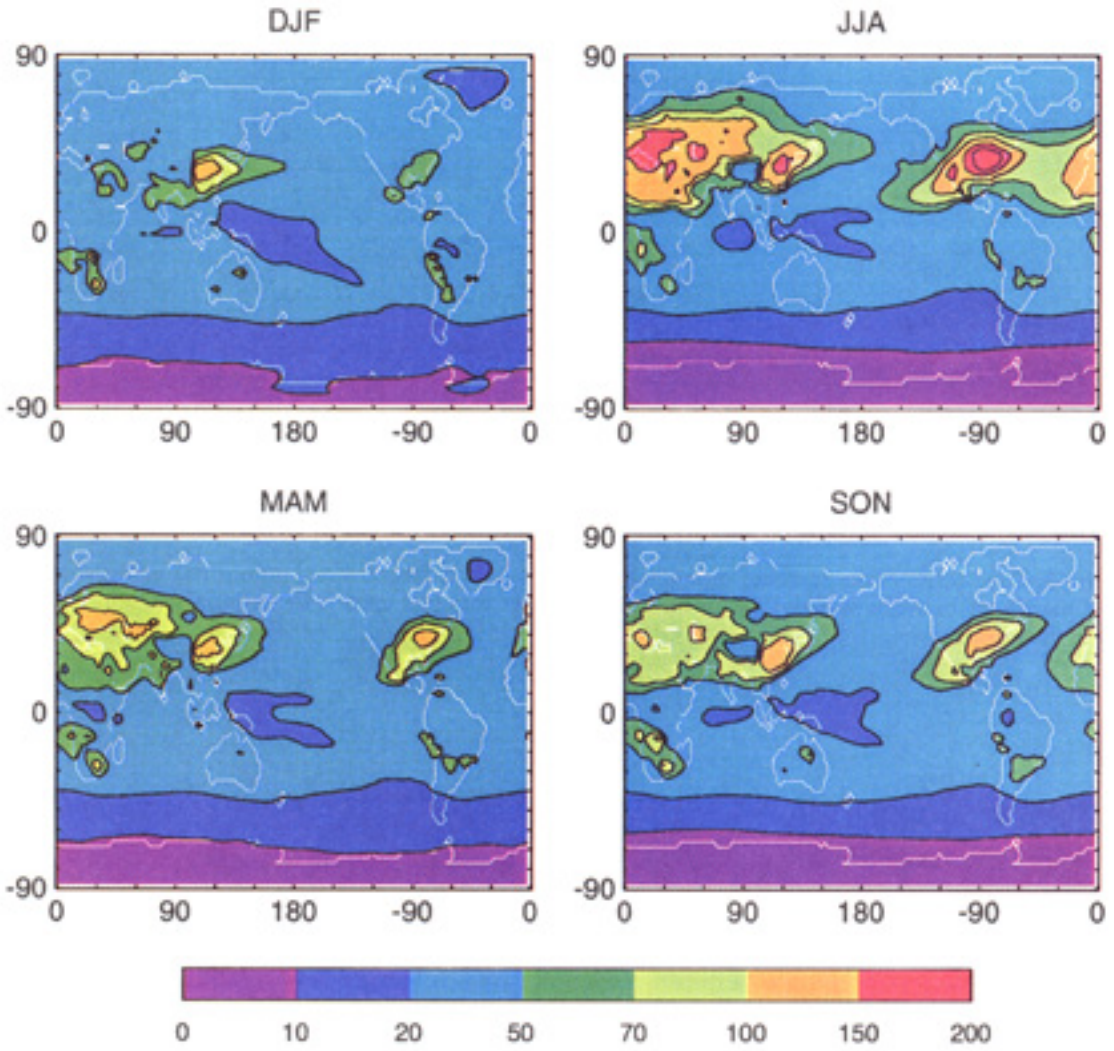

The horizontal distributions of column integrated sulfate for year 3 of our simulations are shown in Plate 2. There are very large seasonal variations in column burdens over the primary Northern Hemisphere emission regions (northeast North America and Europe) and smaller variations over the widely distributed regions of the Southern Hemisphere. The burdens from Asian regions are evident year round. The maxima seen during summer/fall periods are consistent with the time series of Figure 2. We "tag" the emissions and discuss the controlling processes and propogation from each region later in this study.

Explanations for the seasonal cycle of sulfur species concentrations are complex and vary from model to model. Differences in SO_2 emissions (see Figure 1) are relatively small in the GEIA inventory, except over Europe, where they are higher in winter and lower in summer by $\sim \pm 30\%$, in response to variations in power and heat usage. (A similar seasonal cycle was prescribed in the emissions used in the other modeling studies cited here.) During winter, in the presence of a relatively stable boundary layer, concentrations of SO_2 become high, and the transformation of SO_2 to SO_4^{2-} may be locally oxidant-limited. In summer, oxidants are more plentiful, and the venting for the boundary layer can distribute the SO_2 over a larger volume of air, thus exposing it to more oxidant. However, *Langner et al.* [1992] have noted that observational estimates of cloud amounts used in their model are more abundant during winter and spring in the lower and middle troposphere. Since most of the oxidation takes place within clouds, the decrease in cloud amount in summer will act to oppose the increase in the amount of the aqueous oxidants seen in summer.

The analysis of *Feichter et al.* [1996] showed that during summer the role of in-cloud and gas phase oxidation played a nearly equal role in converting SO_2 to SO_4^{2-}, but their net effect was significantly smaller than the wintertime oxidation mechanism, where the in-cloud pathway dominated. In principle this would suggest a minimum in SO_2 in the winter and spring, exactly the opposite of that seen in observations and most model simulations. *Chin and Jacob* [1996] indicated that the supply of H_2O_2 was lowest in winter for their model, implying, in the absence of other controlling processes, an effect opposite to the ECHAM simulations. They

showed that ~80% of the loss of SO_2 from anthropogenically influenced regions occurred in their model through oxidation and deposition mechanisms and explain their seasonal cycle of SO_2 through seasonal variations in the dry deposition velocity (over snow) and the summer/winter difference in oxidation. P. J. Rasch et. al. (A comparison of scavenging and deposition processes in global models: Results from the WCRP Cambridge workshop of 1995; submitted to *Tellus*) showed a strong seasonal cycle in SO_2 in 2 variants of sulfur chemistry in the CCM. One variant used a preliminary, but identical photochemistry to that described in this paper, and the other simply prescribed a uniform oxidation rate of 1.2 days everywhere. Both variants included a seasonally varying deposition velocity sensitive to snow cover and turbulent and convective venting of the boundary layer. Both models showed similar seasonal cycles in SO_2 and SO_4^{2-} burdens, suggesting that the dominant control of the seasonal cycle is not photochemical but due to susceptibility to scavenging. *Kasibhatla et al.* [1997] examined the role of variations in chemical conversion in controlling the seasonal cycle of surface SO_2 and SO_4^{2-}. They noted a seasonal cycle of high sulfate in summer and low sulfate in winter in surface measurements over the United States. Surface measurements in Europe did not exhibit this behavior. They suggested the possibility of a (missing) heterogeneous mechanism for the oxidation of SO_2 that takes place year round as a possible needed pathway to explain these differences in the seasonal cycle of SO_2 and SO_4^{2-} over Europe and North America. Thus seasonal variations in emissions, available oxidant, cloud volume, transport and meteorological processes, and deposition variations all act to modulate the seasonal cycle of SO_2.

In our model the winter maxima in the surface layer in SO_2 in Figure 2 are also exhibited in the layer extending from 500 to 750 hPa. At altitudes above 500 hPa the seasonal cycle in SO_2 is reversed with a maxima appearing in the Northern Hemisphere summer phase, when the SO_2 of surface origin is more easily transported to upper levels. During summer the SO_2 is distributed over a larger volume of air that also has higher oxidant availability making its transformation more rapid.

Further indication of the controlling mechanisms for the seasonal cycle in SO_4^{2-} may be found in Plate 3, which shows profiles of a variety of quantities averaged over all longitudes between 40N and 90N, as a function of η (the model's hybrid vertical coordinate that corresponds approximately to pressure [in hPa]). This domain was chosen to be large enough that lateral transport in and out of the domain does not dominate the signal, and includes the northern hemisphere source regions where the seasonal variations in burden are largest. The Plate 3 (top) shows summertime and wintertime variations in SO_2, SO_4^{2-}, and H_2O_2. SO_2 varies by a factor of 3 between summer and winter in the boundary layer. Peak values are found at ~950 hPa. There is a crossover point at ~400 hPa; above this altitude, summer SO_2 values exceed those in the winter. Below this altitude, wintertime values always exceed summertime values. The seasonal differences in SO_4^{2-} amounts disappear by 100 hPa. Above that altitude, seasonal variations are also modulated by transport into the stratosphere, which is in turn strongly controlled by stratospheric wave drag and is a maximum in the Northern Hemisphere winter. Since this model has low vertical resolution in the stratosphere, and this strongly affects the quality of the simulation there, and because representations of much of the relevant aerosol precursors and physics are missing, we do not focus any more on that region. Below 100 hPa the summer:winter ratio for SO_4^{2-} is ~2:1. H_2O_2 exhibits a very strong seasonal cycle, varying by a factor of 3 between summer and winter. As previously mentioned, the strong maximum in H_2O_2 in summer enhances the aqueous oxidation of SO_2 compared to the winter season. Peak H_2O_2 concentrations during summer occur at ~750 hPa. During winter the peak SO_2 concentrations occur around 400 hPa.

Cloud fraction, total cloud condensate (liquid plus ice) and liquid water are shown in Plate 3 (middle) (the condensate mixing ratios are not in-cloud values but represent averages over the total (clear plus cloudy fraction of the) grid volume. There are significantly more clouds in the model between 900 and 400 hPa during winter than summer. Since the cloud fraction controls the volume where aqueous oxidation can take place, the higher volumes in winter can enhance oxidation during that season compared to summer. On the other hand, there is significantly more liquid water content in summer. Thus the volume of air susceptible to aqueous processing and scavenging is higher in winter than summer, but the mass of water that participates in the chemistry and scavenging is higher in summer than winter.

Plate 3 (bottom) shows the rates of many of the terms involved in the production and removal of sulfate in our model above the surface. Schematically, we represent the sulfate evolution equation as

$$\begin{aligned}\frac{\partial[SO_4^{2-}]}{\partial t} = \quad & \mathrm{ADV} + \mathrm{TURB} + \mathrm{CONV} \\ & + \mathrm{CHEMA} + \mathrm{CHEMG} \\ & + \mathrm{PR} - \mathrm{DRYD} - \mathrm{WETD}.\end{aligned}$$

The right-hand side of the equation represents the net rate (or tendency) associated with individual processes. ADV is the advective tendency, TURB is the net rate of turbulent transport (occuring primarily in the boundary layer), CONV is the rate of convective transport, CHEMA the rate of aqueous oxidation of SO_2 to SO_4^{2-} by O_3 and H_2O_2 , CHEMG is the gas phase oxidation rate, PR is the rate of primary emission of SO_4^{2-}, and DRYD and WETD are the rates of dry and wet deposition processes, repectively. At steady state the left hand side of the equation would be identically zero. Note that we have chosen the sign of the WETD and DRYD terms to appear as positive values on Plates 3 and 4. The positive sign serves to illustrate the very close balance between WETD and other terms (particularly CHEMA) on the figure. Between 950 and 750 hPa, there is a near balance between production from the aqueous pathway and wet deposition during both summer and winter. That is,

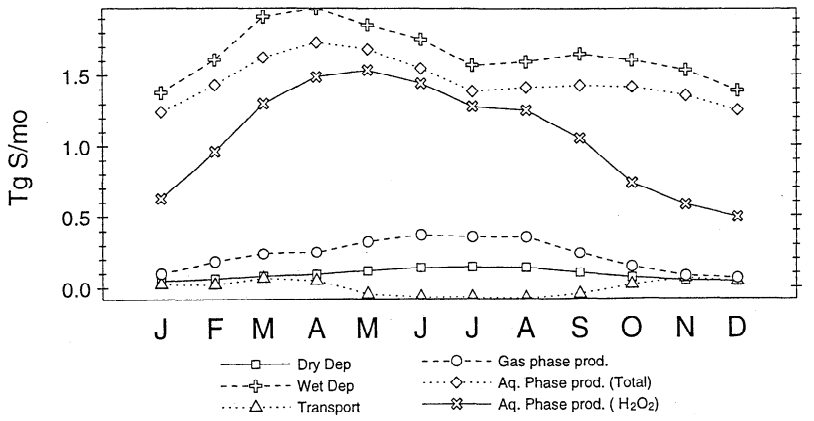

Figure 3. Time series of many of the terms controlling the seasonal variation of sulfate in the atmosphere, averaged over all longitudes between 40°N and 90°N.

$$\text{CHEMA} \approx \text{WETD} \quad 700\,\text{hPa} < \text{P} < 900\,\text{hPa}$$

during both summer and winter. Both processes are more active (by ~20-30%) in our model during winter than during summer in this region, and the aqueous production generally exceeds the wet deposition. The two processes are, of course, intimately tied to one another as much of the sulfate is formed within the cloud in the same event in which it is removed. The excess production over wet deposition is significantly larger in summer than in winter, contributing to the enhanced sulfate burden in summer. Of course, other terms are also important. The gas-phase production (CHEMG) adds significantly to the production excess in summer in this region. At altitudes above 700 hPa and below 900 hPa some aspects of these tendencies are reversed; the aqueous production and wet deposition processes are more active in summer than in winter, and wet deposition dominates the aqueous production. It is also clear that other processes enter into the total balance in both regions. At altitudes above 700 hPa in summer, production by the gas-phase term CHEMG and advection ADV are both important. There is an approximate balance between CHEMA, CHEMG, ADV, and WETD. That is,

$$\text{CHEMA} + \text{CHEMG} + \text{ADV} \approx \text{WETD}$$
$$400\,\text{hPa} < \text{P} < 700\,\text{hPa}$$

in Northern Hemisphere summer. Gas phase oxidation shows a substantial seasonal variation from the surface to 600 hPa. It is higher by 40-50% in summer than in winter. During winter the balance between 400 and 700 hPa is much like the lower altitude region, except that the wet deposition is the largest term and acts to balance all others.

There are a number of surprising results pertinent to the boundary layer region at pressures >900 hPa. Wet (both below- and in-cloud) deposition in the lowest (100 m) layer adjacent to the surface is larger by 30% in winter and 50% in summer than the next higher layer. The aqueous source term (CHEMA), on the other hand, has its maximum in both seasons in the second model layer from the surface (100-300 m). This is probably due to the maxima in cloud water and cloud fraction seen in Plate 3 (middle), and because SO_2 emissions are above 100 m are as large or larger than as those at the surface. Convective transport (CONV) and turbulent transports (TURB) of aerosol are both important in the boundary layers with large positive amplitudes in the near surface layer, and negative values higher up. Thus these terms act to transport aerosol from higher levels downward and into the surface layer where it is susceptable to strong removal by dry deposition processes (not shown) and wet scavenging. Convective transports are usually thought to act to move constituents out of the boundary layer. In the case of soluble species, however (at least as represented here),

Table 2. Global Annual-Averaged Dimethlysulfide (DMS) Budgets for Years 3-6 Compared to Other Model Studies

Quantity	LR91	P95	F96	C96	L97	This work
Source Tg S/yr	16	20	17	22	16	16
Burden Tg S	0.13	0.05	0.10	0.06	0.02	0.06
Lifetime Days	3	0.9	2.2	1.0	0.5	1.42

Previous studies are abbreviated as follows: LR91, *Langner and Rodhe* [1991]; P95, *Pham et al.* [1995]; F96, *Feichter et al.* [1996]; C96, *Chin et al.* [1996]; and L97, *Lelieveld et al.* [1997].

Table 3. Global Annual-Averaged SO_2 Budgets for Years 3-6 Compared to Other Model Studies

Quantity	LR91	P95	F96	C96	L97	This work
Source Tg S/yr	95	123	101	96	90	79
Anthro. emissions %	71	75	78	68	74	82
Photochemical prod. %	18	15	17	23	18	18
Other %	11	10	6	9	8	0
gas-phase oxidation %	8	5	17	8	15	12
In-cloud oxidation %	44	45	34	44	59	56
Wet deposition %	15	4	9	21	0	2
Dry deposition %	32	45	40	28	24	31
Burden Tg S	0.3	0.2	0.4	0.3	0.6	0.4
Lifetime Days	1.2	0.6	1.5	1.3	2.3	1.9

Previous studies are abbreviated as follows: LR91, *Langner and Rodhe* [1991]; P95, *Pham et al.* [1995]; F96, *Feichter et al.* [1996]; C96, *Chin et al.* [1996]; and L97, *Lelieveld et al.* [1997].

the upward transport inside the updraft cores of any aerosol remaining after scavenging, is overwhelmed by the compensating downward transports of unscavenged aerosol in the environment. Advection (ADV) by resolved-scale processes (i.e., not turbulence) generally acts to move the sulfate from the near-surface layers both upward and laterally (in this case southward). During the summer, advection acts as a significant source to the region from 700 to 500 hPa. During winter it acts mostly to move SO_4^{2-} out of the domain. Within cloudy volumes nonadvective processes dominate the advection term, but in cloud free regions advection is important, and its enhanced role in summer time must be due to the larger volume of cloud-free air during that season.

The column integral of each term for the same domain are shown in Figure 3 on a month by month basis. The seasonal variation of these quantities shows interesting differences with the corresponding quantities shown by [*Feichter et al.*, 1996, Figure 1] . Their simulations indicated a maximum in oxidation via H_2O_2 in March and April, and a minimum (of 0.7 Tg S/month) in June and July. The present model exhibits a similar maximum, but the minimum in June, July, and August (JJA) is much smaller than the simulation of Feichter et. al. The shape of the seasonal cycle in the gas phase production of Feichter et al. is quite similar to the present model, but their maximum in summer is approximately twice as large as that found here. Feichter et al. found a maximum in surface deposition in the fall, where the maximum is in the spring in the present model. The differences in the 2 models' portrayal of seasonal variations in processes again highlight our current uncertainty in understandings of the atmospheric sulfur cycle.

When the region of integration is restricted to the region of strongest emissions, the balances change, compared to the larger Northern Hemisphere region. Plate 4 shows the corresponding profiles over eastern North America. As should be anticipated, the vertical gradient of SO_2 and SO_4^{2-} is larger over the source region, and near-surface values are a factor of 2 higher. Summertime values of SO_2 are higher than wintertime values at all altitudes above 800 hPa. The mass of liquid condensate is substantially lower over this area than over the Northern Hemisphere in general. Unlike the larger region, there is more total condensate in winter than in summer, although there is still much more liquid condensate in summer than in winter. The difference between summer and winter cloud fraction is also much larger. All tendencies tend to be a factor of 2 higher in the smaller source region than averaged over the larger domain. Lateral advection of sulfate out of the domain is also more apparent. There is a net vertical transport into the region from 500 to 700 hPa by resolved-scale advection from below. As is also seen over the larger region, the gas-phase oxidation shows a substantial seasonal variation from the surface to 600 hPa. It is higher by 40-50% in summer than in winter. This result differs from a similar analysis in the model study of *Chin and Jacob* [1996], who

Table 4. Global Annual-Averaged SO_4^{2-} Budgets for Years 3-6 Compared to Other Model Studies

Quantity	LR91	P95	F96	C96	L97	This work
Source Tg S / yr	53	62	51	49	72	55
Anthro. emissions %	6	0	0	0	5	2
gas-phase production %	15	10	33	15	21	17
In-cloud production %	79	90	67	85	74	81
Dry deposition %	16	27	13	11	25	7
Wet deposition %	84	73	87	89	75	93
Burden Tg S	0.8	0.8	0.6	0.53	1.1	0.60
Lifetime Days	5.3	4.7	4.3	3.9	5.3	4.0

Previous studies are abbreviated as follows: LR91, *Langner and Rodhe* [1991]; P95, *Pham et al.* [1995]; F96, *Feichter et al.* [1996]; C96, *Chin et al.* [1996]; and L97, *Lelieveld et al.* [1997].

found no variation in the rate of summer and winter production of sulfate by gas-phase photochemistry in the lower troposphere. The difference between summertime and wintertime production by aqueous oxidation is also substantially larger over this region than over the larger domain discussed above. Both sulfate and SO_2 are transported to the middle and upper troposphere by convection, despite their solubility, and the convection term is significantly larger over this (primarly) continental region than it is over the larger domain. Convection and oxidation of SO_2 by OH are sources for sulfate between 200 and 500 hPa in summer. These source terms for sulfate at heights above 500 hPa are balanced by advection, which acts to transport the sulfate elsewhere. Between the surface and 700 hPa, sources of SO_4^{2-} by aqueous and gaseous oxidation substantially (by $\sim$100%) exceed the wet deposition process; the remaining excess of production is exported from this region by advective processes, particularly during summer.

Global budgets for the present model and several other recent model studies are shown in Tables 2-4. These studies are certainly not a comprehensive list, but they provide a general picture of the current range of variation in global modeling. Three of the models [*Langner and Rodhe*, 1991; *Pham et al.*, 1995; *Chin et al.*, 1996] are off-line models characterized by relatively simple formulations for transport, convection, and cloud processing, necessitated by the lack of much of the information required for a more elaborate formulation (none of these models had access to three-dimensional distributions of cloud variables, for example). The studies of *Feichter et al.* [1996] and *Roelofs et al.* [1998] are quite similar to ours. They also utilized a GCM in which the model hydrological cycle, cloud volumes for chemical processing, etc., were handled on short time-scales in an internally consistent way. Some of the prior studies included additional source terms (volcanoes and biomass burning) neglected in our study. On the other hand, some of the cited studies have treated a smaller number of oxidation pathways (for example, by neglecting reactions with O_3). Only the models described by *Lelieveld et al.* [1997] and *Roelofs et al.* [1998] have as elaborate a treatement of the production and loss of H_2O_2.

The lifetime of DMS (Table 2) varies considerably among the several models. *Langner and Rodhe* [1991] did not include the NO_3 oxidation pathway, and assumed all DMS + OH went to SO_2. Their lifetime is the longest of the cited models. *Chin et al.* [1996] postulated and used a missing oxidation path for DMS in order to achieve a reasonable agreement with observations. The additional pathway reduced the DMS lifetime substantially. It is interesting to note that the studies of *Feichter et al.* [1996] and *Lelieveld et al.* [1997], which use the same fundamental meterological description and aerosol chemistry, differ by a factor of 4 in the DMS lifetime (2.2 versus 0.5 days, respectively). The difference is presumably due to variation in OH distributions. The present model lies between those model results.

With respect to SO_2 the present study, which lacks volcanic emissions, biomass burning, and CS_2 and COS sources has the lowest source strength for SO_2, and thus anthropogenic emissions appear as a relatively higher fraction of the source in Table 3. The three models using a prognostic cloud water variable, and interactive clouds tend to lose more SO_2 by gas-phase oxidation than the models containing simpler formulations for clouds. These studies also limited the SO_2 oxidized by H_2O_2 more strictly than the studies of *Chin et al.* [1996] and *Pham et al.* [1995]. There is an order of magnitude of variation in wet deposition of SO_2 between models, ranging from the present study, *Lelieveld et al.* [1997] and *Roelofs et al.* [1998] at the low end (2% and 0% respectively) to that of *Chin et al.* [1996] at the high end (21%). This is likely to be a explained as a labeling issue. The partitioning of the SO_4^{2-} that has not yet existed as an aerosol [S(VI)] can be distinguished from that arising from ingestion of a preexisting soluble aerosol by a precipitating cloud drop. Our wet deposition of SO_2 refers only to the deposition of S(IV). The balance is attributed to deposition as sulfate. As such, our numbers are quite consistent with the numerous observational estimates cited by *Wojcik and Chang* [1997]. Part 1 (Figure 3) suggests that our model agrees quite well with observations of total wet deposition (SO_2 + SO_4^{2-}) and thus the discrepancy among models is likely just a labelling issue. *Langner and Rodhe* [1991] also included the enhanced uptake of SO_2 in solution due to complexation with formaldehyde. The sum of wet deposition and aqueous oxidation provides an estimate of loss of SO_2 through cloud processing. There is still a large variation between these fields among models, and the 2 models with the most internal consistency in treatment of physical processes are very different in this sense (43% versus 58% respectively). The 2 models with predicted H_2O_2 distributions have the longest lifetime for SO_2. The depletion of H_2O_2 in near-source regions can result in a decrease in the rate of production of SO_4^{2-}. Part 1 showed that there was often an appreciable length of time for replenishment of the H_2O_2 after it was depleted through oxidation and precipitation scavenging. This would increase the frequency of situations where SO_2 is limited to the slower O_3 reaction for its oxidation pathway. (Not allowing the H_2O_2 depletion results in an increase of order 7% in the production of SO_4^{2-}.)

Despite the large differences in emission inventories, photochemistry, cloud properties, and deposition parameterizations for SO_2, the net source for SO_4^{2-} from all the models varies by only 20% (Table 4), with the exception of the model described by *Lelieveld et al.* [1997] and *Roelofs et al.* [1998], which has a signifiantly higher source value. The partitioning between aqueous- and gas-phase production varies substantially between models. All models show the aqueous pathway to dominate, but there is no consistent signature between models with the more elaborate treatments for clouds and oxidation and the simpler formulations. This suggests, again, that there are still very large uncertainties in the characterization of the atmospheric sulfur cycle.

4. Regional Analysis

It is now generally accepted that emissions from the industrial nations of the Northern Hemisphere are the domi-

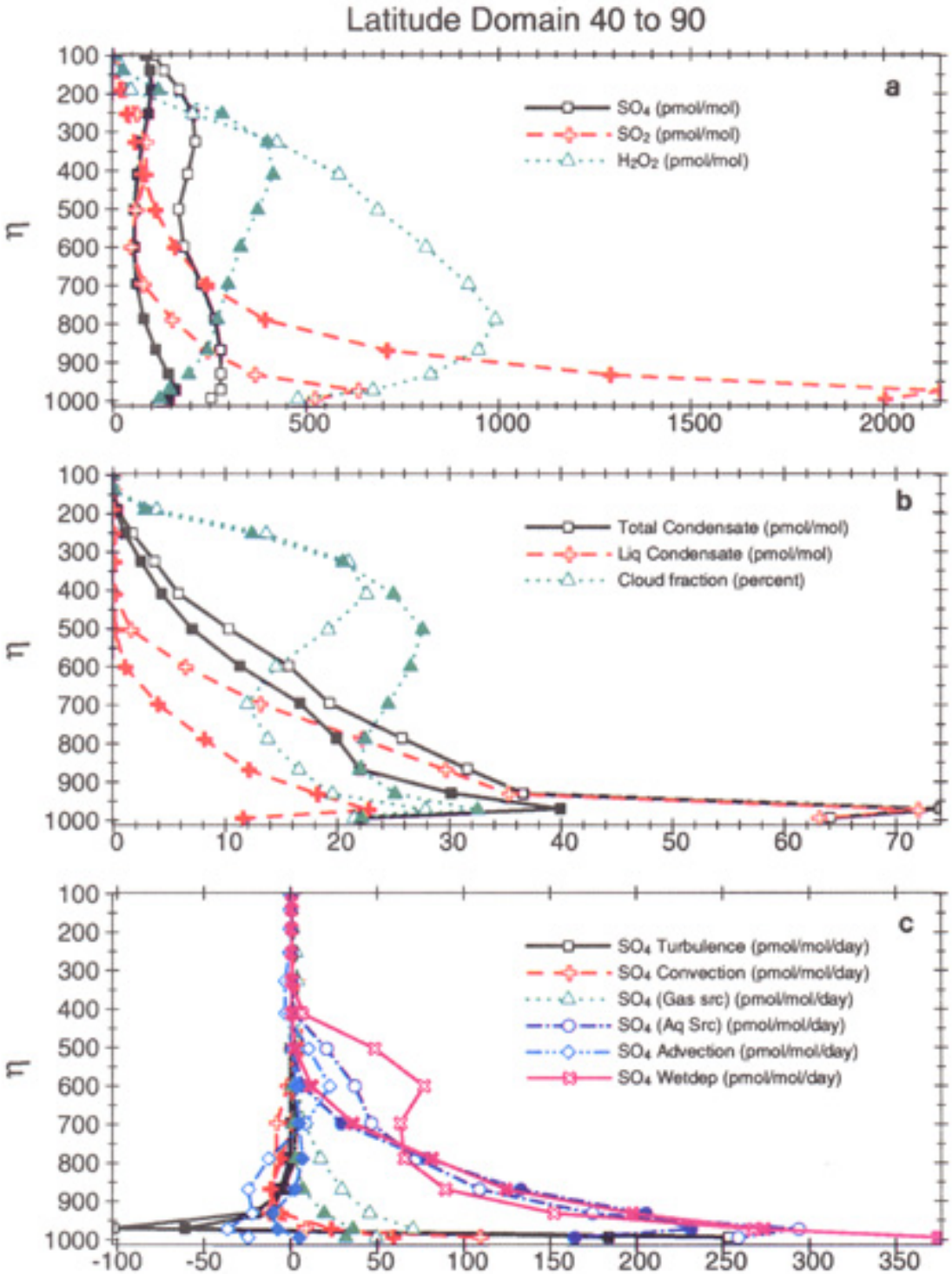

Plate 3. Profiles of many of the terms controlling the seasonal variation of sulfate in the atmosphere, averaged over all longitudes between 40°N and 90°N. The open markers show the summertime, and the solid markers the wintertime values. The vertical coordinate η corresponds approximately to hPa. Note that we have chosen the sign of the wet deposition term to appear as a positive value to emphasize the balance between deposition and production.

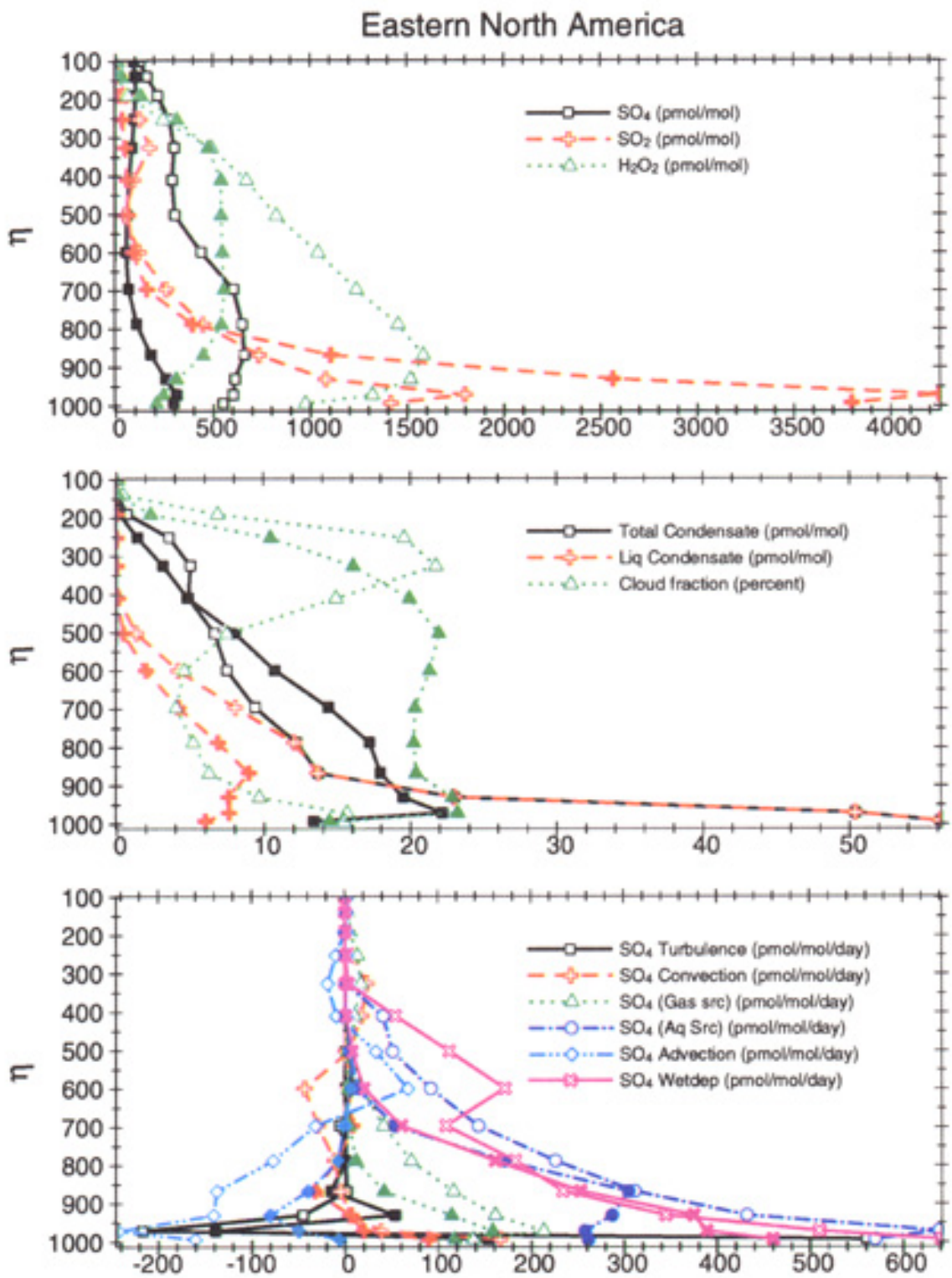

Plate 4. Profiles of many of the terms controlling the seasonal variation of sulfate in the atmosphere, averaged over eastern North America (60°W-90°W, 30°-60°N). The open markers show the summertime values, and solid markers the wintertime values. The vertical coordinate η corresponds approximately to hPa.

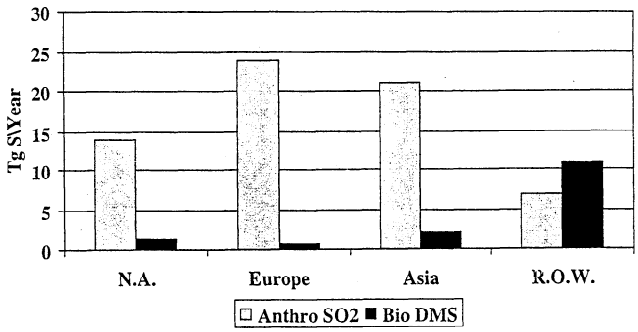

Figure 4. Annual emission of sulfur speciecs by region, partitioned by anthropogenic and biogenic emissions.

nant source of tropospheric sulfate in the world today. Yet the relative contribution of the several source regions to the global sulfur budget and possible differences in the processes that control the sulfur distribution from these regions remain poorly understood. In this section we make use of tagged aerosol types to make infererences about the effect of emissions from the different regions.

The partitioning of the annually averaged regional emissions and burdens into their anthropogenic and biogenic components can be assessed from the bar charts of Figures 4 and 5. Anthropogenic emissions dominate over biogenic emissions in all regions except ROW, where they are of similar magnitude. In the Northern Hemisphere more than 80% of the total burden is due to anthropogenic sulfate. However, even in the Southern Hemisphere, the anthropogenic sulfate is generally more than 50% of the total burden. In the tropical region of the Pacific Ocean, sulfate aerosols derived from DMS emissions and anthropogenic sulfate contribute equally to the total burden. These results contrast with the result of *Chin and Jacob* [1996], who found a larger contribution from nonanthropogenic sources, particularly in the Southern Hemisphere and oceanic regions. These differences could arise because in our model, DMS emissions are less than those used by *Chin and Jacob* [1996] and because our model does not include volcanic emissions of SO_2, or because *Chin and Jacob* [1996] determined the anthropogenic contribution by comparing simulations using only natural emissions to a simulation with present-day natural and anthropogenic emissions. We have also made similar preindutrial and present-day runs, and we believe that most the differences between our simulations and those of *Chin and Jacob* [1996] cannot be explained by the non-linear reponse of the chemistry and scavenging to the changing emissions.

Although the ratio of anthropogenic to biogenic emissions in the Northern Hemisphere regions of Europe, North America, and Asia are approximately 10:1 or greater, the burdens of resulting sulfate are of order 5:1 for the corresponding regions. That is, the yield of sulfate is higher from biogenic precursor emissions than from anthropogenic precursors. Hence sulfur emitted from biogenic sources is converted to sulfate (relatively) more efficiently than that emitted from anthropogenic sources. This is easily explained [*Chin and Jacob*, 1996; *Feichter et al.*, 1997] by the rapid transport from the surface to the upper troposphere of the quite insoluble DMS, where it is subsequently oxidized to SO_2 and SO_4^{2-}. Sulfate produced in the upper troposphere is not easily susceptable to scavenging, and must first be transported downward to altitudes where removal processes are more efficient. It is also evident from Figure 5 that there are significant differences between the relative partitioning between SO_2 and SO_4^{2-} among the regions. While there is more sulfur stored as SO_4^{2-} in the North America, Asian, and ROW regions, the situation is reversed in Europe. These features suggest significant differences in transport, transformation, and deposition mechanisms over the four regions (discussed below).

The point can be made more strongly by considering what we term the "potential" or "susceptability" of a region to emissions. This is defined to be

$$\text{potential} = \frac{\text{SO}_4 \text{ aerosol burden}}{\text{near surface sulfur emission}}.$$

Thus the sulfate potential defines the yield of aerosol per unit emisssion of sulfur as SO_2 or DMS.

Figure 6 shows that anthropogenic emissions from ROW have more potential for aerosol formation than other regions. A kilogram of sulfur emitted as SO_2 from a ROW source will produce ~4 times more aerosol than the same kilogram

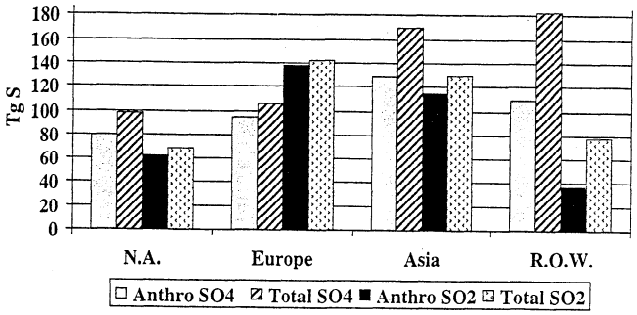

Figure 5. Annually averaged burden of sulfur species by region, partitioned into anthropogenic and total contributions.

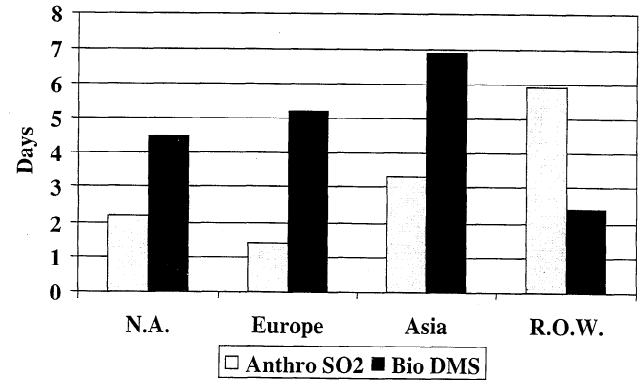

Figure 6. Sulfate potential, defined as the sulfate burden (Kg S) resulting from a unit emission of sulfur (Kg S/day) at the surface.

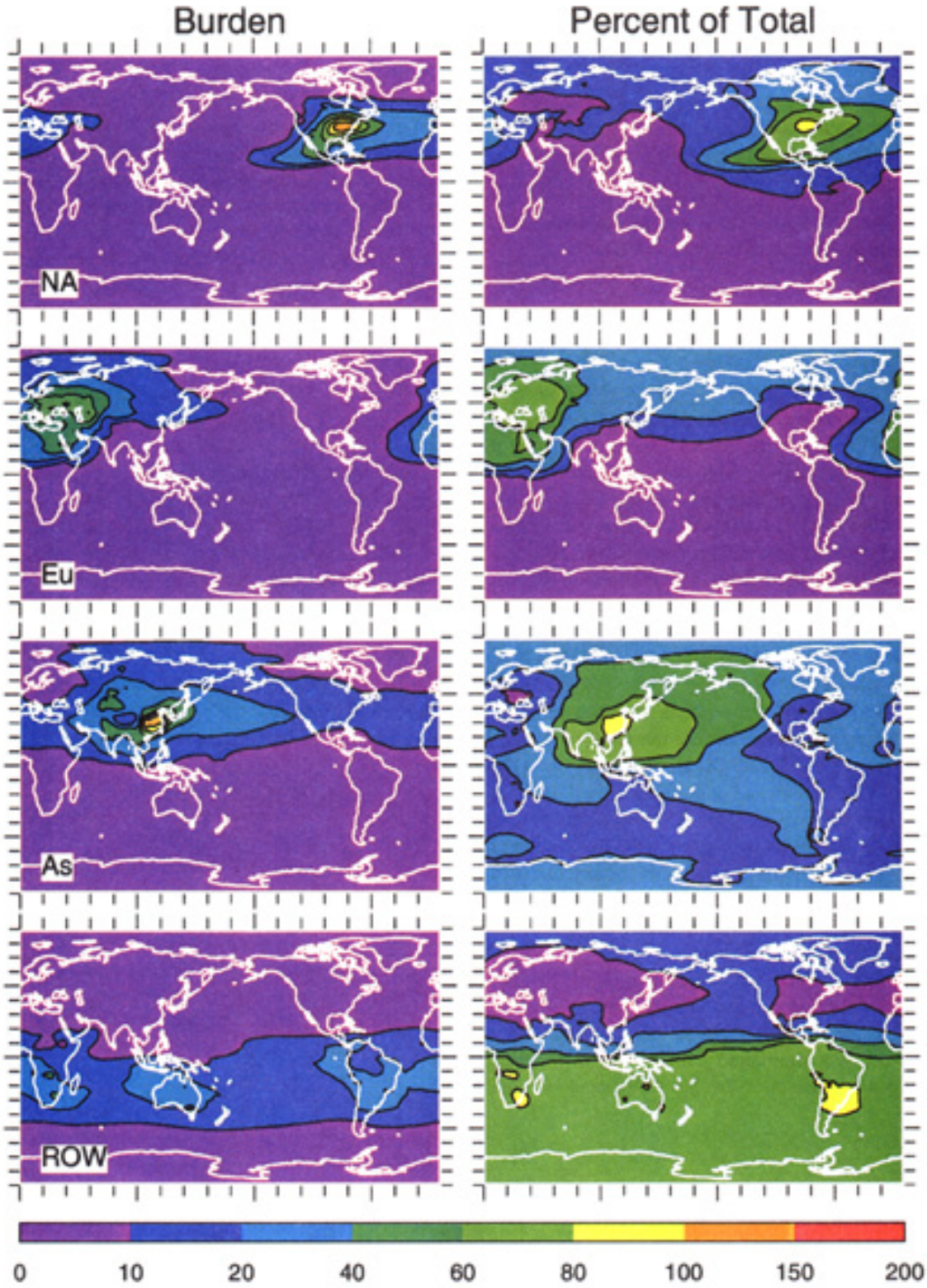

Plate 5. Annual-averaged column burden of sulfate for the four regional emissions (left) in μmol/m^2, and (right) as a percent of the total burden.

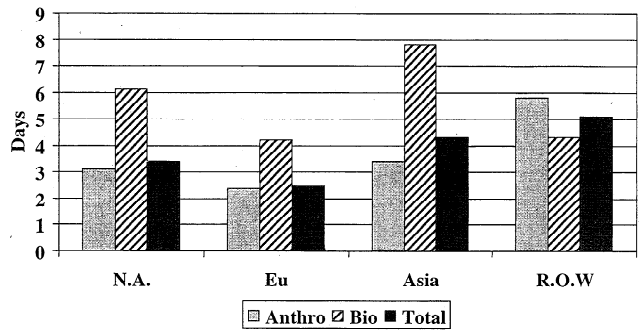

Figure 7. The lifetime of sulfate emitted from each region.

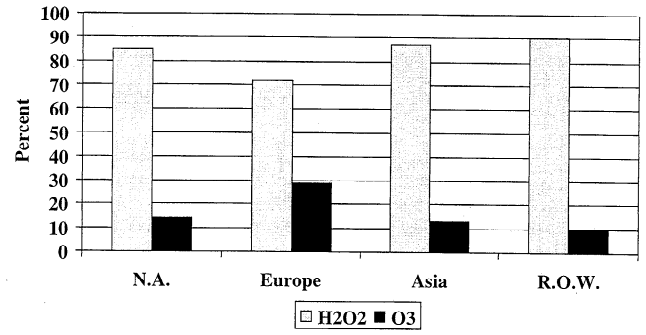

Figure 9. The fraction of oxidation taking place by the 2 primary aqueous-phase pathways.

of SO_2 emitted over Europe, which has the lowest potential for sulfate formation according to our model. The Asian region is intermediate to the others in this susceptibility to aerosol formation. The sulfate potential does not identify what process or processes control the distribution and amplitude of the aerosol mass, it just defines the potential for a given emission of a sulfur atom from a region to end up as sulfate mass.

The controlling processes can be identified by a consideration of ratios of other quantities available from the model. Figure 7 shows the sulfate lifetime (defined as the ratio of the sulfate burden to the total deposition flux). This quanitity is the inverse of the rate at which sulfate (arising from emissions from a given region) is removed from the atmosphere. The diagnostic suggests that part of the explanation for the potential is associated with deposition processes. Sulfate arising from anthropogenic ROW sources has a lifetime against deposition of ~6 days and is not deposited as readily as sulfate from other regions at the surface. Also, unlike the other regions, the lifetime of biogenic sulfate from that region is actually shorter than that of the anthropogenic component. The vertical distribution of the anthropogenic ROW sulfate is nearly uniform, somewhat like DMS and thus ROW aerosols are not so susceptible to scavenging. We believe that this is because the ROW sources are in close proximity to regions of vigorous continental year-round convection (e.g., Amazonia and South Africa) that transport the SO_2 rapidly to the upper troposphere.

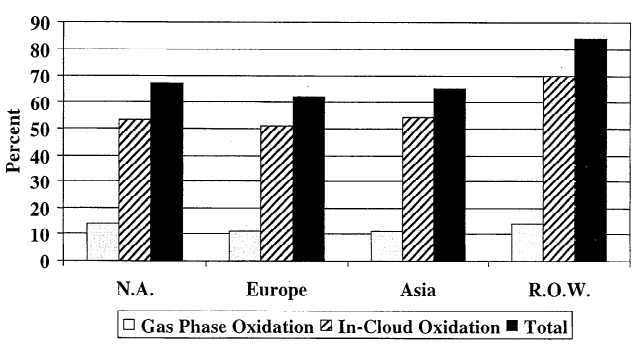

Figure 8. The fraction of SO_2 emitted from each region that is converted to SO_4^{2-}.

Figure 8 shows the sulfate yield as a fraction of emitted SO_2 that produces sulfate. The balance of the SO_2 undergoes wet or dry deposition. ROW SO_2 emissions result in a 15-20% greater yield than do emissions from other regions. This total yield can, in turn, be partitioned into aqueous- and gas-phase oxidation components. Thus ROW sources are converted more efficiently to sulfate and are subject to less efficient surface deposition than other regions. Also, the ratio of aqueous to gaseous oxidation is also slightly higher in ROW than other regions.

Figure 9 partitions the aqueous oxidation pathways according to the fraction oxidized by H_2O_2 or O_3. Europe stands out from the other regions by having a much higher (factor of 2) fraction of the sulfate produced by the O_3 pathway. This suggests that the European region exists in a peroxide limited situation much more frequently than any of the other model regions. This can be attibuted to the much higher emissions densities over Europe compared to any of the other defined areas. Also, because Europe is located at higher latitudes than the other regions, there is less oxididant availability, and reaction rates are slower. This effect is most pronounced in winter when the European emissions peak.

5. Spatial and Seasonal Distributions From Regional Emission

The horizontal spatial distribution of each of the annually averaged regionally tagged sulfate types are shown in Plate 5. Plate 5 (left) shows the column burden from each emission region, and Plate 5 (right) the percent of the total column burden contributed from each region. In the interest of brevity we do not show, but will discuss, the seasonal variation of the regionally tagged sulfate. There is a strong seasonal variation for Europe and North America, with summer to winter ratios peak values of ~4:1 over both regions. The plume emitted from North America extends eastward following the storm track and carries a factor of ~two more sulfate over the Atlantic in summer than in winter. The peak amplitudes over the North American and European emission regions are quite similar to those described by *Feichter et al.* [1996] and *Kasibhatla et al.* [1997]. Another plume from the southwest United States and Mexico areas is also evident during summer. The plume (also seen by *Benkovitz*

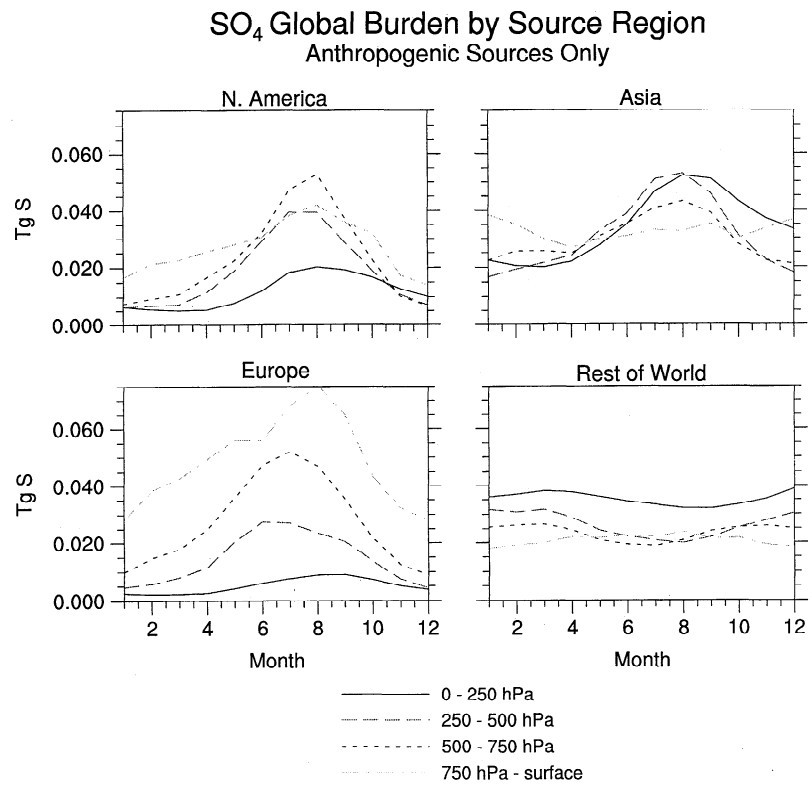

Figure 10. Time series for year 3 of the sulfate burden stratified by layer for each region.

et al. [1994]) extends westward in the subtropics and carries significant amounts of sulfate across the pacific as far as Hawaii. This plume is significantly stronger than that seen by *Feichter et al.* [1996]. The model evaluation of part 1 suggests it is probably too strong. The Asian emissions generate burdens that are quite similar to those seen by *Feichter et al.* [1996] but significantly greater than those seen by *Kasibhatla et al.* [1997]. There is little seasonal cycle in maximum amplitude but the extent of the area occupied by a high sulfate burden is significantly larger in Northern Hemisphere summer than in winter. There are much smaller variations between summer and winter burdens from the ROW emissions. Burdens of 60 μmol/m^2 during summer are a factor of 2 larger than during winter.

The picture changes somewhat when viewed as a percentage. Asian emissions (including those from Siberia) contribute most strongly to burdens in the Northern Hemisphere polar regions during winter; during summer, European sources contribute most strongly. North America appears as a distant third place contributor in all seasons. Very little (<10%) of the sulfate derived from emissions from North America or Europe penetrate into the Southern Hemisphere. Similarly, very little of the sulfate from ROW emissions penetrate into the Northern Hemisphere. Asia, on the other hand contributes in an important way to the burden in both the Northern and Southern Hemispheres. It reaches the Southern Hemisphere most efficiently in the JJA season where it comprises 20-40% of the burden in the subtropics. Although this contribution to the Southern Hemisphere is quite small in magnitude, it indicates a pathway for transport from anthropogenic sources of potential importance in the future. The ROW sources reach to ~30N during Northern Hemisphere winter, where they comprise ~30% of the column burden there.

Seasonal cycles of the SO_4^{2-} burdens in each vertical quartile (250 hPa layer) are shown in Figure 10 for each emission region. The largest burdens result from European emissions with summer to winter ratios of ~2:1. Burdens from European emissions fall off with increasing altitude more strongly than any of the other regions. Asian and ROW burdens have the least seasonality and stratification.

Latitude-height cross-sections of zonally averaged sulfate from each region are shown in Figure 11. The largest lower tropospheric values are associated with the European emission region during Northern Hemisphere summer. The sulfate aerosol remains at low altitudes for the European source region, in contrast to a penetration of relatively large sulfate loadings to higher altitudes from North American and Asian sources. The Asian source emission contribute the most to the north polar region during Northern summer. The ROW source emissions are much more uniformly distributed in the vertical and show little seasonal variation. The emission regions associated with areas of vigorous deep convection tend to have significantly higher burdens aloft. The sulfate from all source regions shows a spreading of contours with altitude, indicating that once aloft, the aerosol is less susceptable to removal processes and so can travel great distances unimpeded. This tendency is evident for each distribution

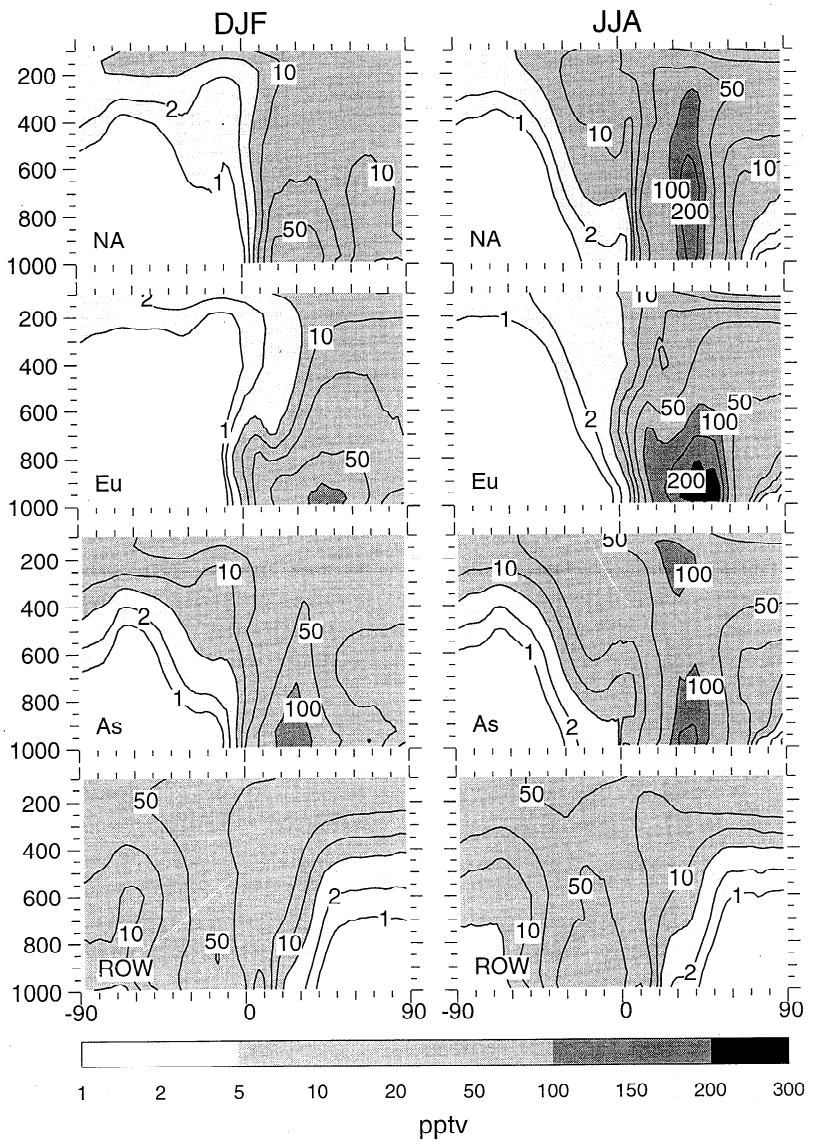

Figure 11. Zonal average of sulfate distribution for the four regional emissions (biogenic plus anthropogenic, regions are indicated in the lower left) for DJF (left column) and JJA (right column).

of Figure 10. Asian emissions are most important to the supply of upper tropospheric sulfate in the Northern Hemisphere, and Asia is the only important Northern Hemisphere source region reaching to the Southern Hemisphere. The Asian source region is responsible for more than 40% of the sulfate above 400 hPa in the Northern Hemisphere. North American and European sources are trapped in the Northern Hemisphere and contribute <10% to the aerosol amount at any altitude in the opposite hemisphere.

6. Summary and Conclusions

We have examined the balance between processes that contribute to the global and regional distributions of sulfate aerosol in the Earth's atmosphere using a set of simulations from the NCAR CCM3. The model, the sensitivity to its chemical formulation, and the comparisons to observations are described in detail in part 1 [*Barth et al.*, this issue]. The radiative forcings that arise from these simulations are analyzed in Part 3 [*Kiehl et al.*, 1999].

The analysis suggests that the seasonal cycles of SO_2 and SO_4^{2-} are controlled by a complex interplay between transport, chemistry, and deposition processes. The seasonal cycles of these species are only weakly influenced by seasonal variations in emissions. Rather, they are controlled by seasonal variations in the volume of air processed by clouds, by mass of liquid water serving as a site for aqueous chemistry, by amount of oxidant available for the conversion from SO_2 to SO_4^{2-}, and by variations in vertical precipitation and transport processes. Three separate processes contribute to vertical transport: (1) advective processes resolved by the present model, (2) transport by subgridscale convection, and (3) transport by subgridscale turbulent processes in the boundary layer. The primary removal mecha-

nism for sulfate is wet deposition. Both the gaseous and the aqueous production of aerosols are substantially higher in the summer in the lower troposphere (surface to 3 km) than in winter. The enhancement is probably due to more clouds in the liquid phase and higher oxidant concentrations. Wet deposition has a strong seasonal variation in the near-surface layer (surface to ~1km) but very little variation between 1 and 3 km. The excess production between 1 and 3 km leads to an enhanced burden at these altitudes. At higher altitudes, the balance of processes becomes more complex, with vertical transport processes also playing a role. There is significant convective transport of SO_2 and SO_4^{2-} during summer. Resolved-scale advection in cloud-free areas also plays a role during summer but not during winter. This suggests that the resolved vertical advection during summer is taking place in the cloud-free regions (which are larger in summer); in cloudy regions the wet deposition tends to reduce the importance of the resolved vertical transport. The seasonal behavior and balance of processes in our model differ in many ways from those found in model studies by *Feichter et al.* [1996] and *Chin and Jacob* [1996]; we do not believe that there are sufficient measurements to identify which of these studies is most realistic. The differences highlight the uncertainty in the processes responsible for sulfate's seasonal behavior. More work is need to resolve these discrepancies.

A tagging of the aerosol by emission region (Europe, North America, Asia, and ROW), chemical pathway (gaseous versus aqueous), and type of emissions (anthropogenic versus biogenic) was used to differentiate the balance of processes controlling the aerosol resulting from the emissions. The analysis suggests that significant differences exist in the destiny of SO_2 emitted from these various regions. An SO_2 molecule emitted from the ROW source region has a much greater potential to contribute to the burden of atmospheric sulfate than one emitted from, for example, Europe. This is due to a number of factors. A greater fraction of the SO_2 molecules originating from ROW are oxidized compared with other areas, and once formed, the aerosol has a longer residence time (that is, it is less readily scavenged, because it has been transported to regions where scavenging is less important). This statement can be quantified in terms of the sulfate potential. The ROW potential (or susceptibility) is a factor of 4 greater than that of Europe (which is the region with the lowest sulfate potential). The ROW region emissions are low compared to the other three source regions, but the region generates burdens of comparable magnitude to that from the other source regions having much greater sulfur emissions.

Other differences between regions are also evident from the analysis. A substantially greater fraction of the SO_2 emitted over Europe is oxidized to SO_4^{2-} through the ozone pathway than from any of the other regions. The large emissions in a limited area lead to larger concentrations of SO_2 than in any other region. In this situation, there is not enough H_2O_2 to oxidize all the SO_2, and the importance of the O_3 reaction increases. These situations are encountered much less frequently in other areas of the world, where SO_2 concentrations are lower and oxidant concentrations are higher.

The analysis suggests that there are also differences among the several source regions in the vertical distribution and horizontal extent of the propagation of the emissions. near-surface SO_4^{2-} amounts generally originate from local source regions, but at higher altitudes the sulfate may originate from very distant sources. Sulfate from the Asian emissions reach the farthest from their point of origin. They make a noticable contribution to burdens in both hemispheres, primarily from plumes reaching out in the middle and upper troposphere. For example, perhaps 50% of the sulfate occuring on the west coast of the United States in summer originates from Asian emissions. SO_4^{2-} from the ROW sources remains trapped, primarily in the Southern Hemisphere. Similarly SO_4^{2-} from North American and European emissions remains primarily in the Northern Hemisphere.

If these conclusions are robust, they suggest that some caution needs to be used in planning for future emissions in regions with high aerosol potential. To zeroth order the burdens generated from these emission will have a corresponding effect on other climate factors (e.g., direct radiative forcing), although the strong sensitivity in aerosol optical properties to relative humidity means that aerosols near the surface may have a larger direct radiative effect than those located at higher altitudes. The situation is not so straightforward when one considers the possibility of the aerosols influencing the climate indirectly (either through changes to the clouds albedos or to their microphysical properties). The indirect effects occur primarily in liquid phase clouds. If changes in the emissions result in changes to upper tropospheric aerosol amount, then this will have little influence on the drop size of liquid clouds and thus little influence on cloud albedo or lifetime.

Acknowledgments. We would like to thank Susan Solomon and Henning Rodhe for numerous discussions that helped clarify ideas discussed in this manuscript. We thank Brian Eaton for programming assistance. Work at BNL was supported by the Environmental Sciences Division of the U.S. Department of Energy and was performed under contract DE-AC02-98CH10886.

References

Albrecht, B., Aerosols, cloud microphysics and fractional cloudiness, *Science*, *245*, 1227–1230, 1989.

Asselin, R., Frequency filter for time integrations, *Mon. Weather Rev.*, *100*, 487–490, 1972.

Barth, M., P. J. Rasch, J. T. Kiehl, C. M. Benkovitz, and S. E. Schwartz, Sulfur chemistry in the National Center for Atmospheric Reseach Community Climate Model: Description, evaluation, features and sensitivity to aqueous chemistry, *J. Geophys. Res.*, 1998, this issue.

Benkovitz, C., C. M. Berkowitz, R. C. Easter, S. Nemesure, R. Wagener, and S. E. Schwartz, Sulfate over the North Atlantic and adjacent continental regions: Evaluation for October and November 1986 using a three-dimensional model driven by observation-derived meteorology, *J. Geophys. Res.*, *99*, 20,725—20,756, 1994.

Benkovitz, C., M. Scholtz, J. Pacyna, L. Tarrason, J. Dignon, E. Voldner, P. Spiro, J. Logan, and T. Graedel, 1995 global gridded inventories of anthropogenic emissions of sulfur and nitrogen, *J. Geophys. Res.*, *101*, 29,239—29,254, 1996.

Charlson, R. J., S. E. Schwartz, J. M. Hales, R. D. Cess, J. A. Coak-

ley, J. E. Hansen, and D. J. Hofmann, Climate forcing by anthropogenic aerosols, *Science*, *255*, 423—430, 1992.

Chin, M., and D. Jacob, Anthropogenic and natural contributions to tropospheric sulfate: A global model analysis, *J. Geophys. Res.*, pp. 18,691—18,699, 1996.

Chin, M., D. J. Jacob, G. M. Gardner, M. Foreman-Fowler, P. A. Spiro, and D. L. Savoie, A global three dimensional model of tropospheric sulfate, *J. Geophys. Res.*, pp. 18,667—18,690, 1996.

Chuang, C. C., J. E. Penner, K. E. Taylor, A. S. Grossman, and J. J. Walton, An assessment of the radiative effects of anthropogenic sulfate, *J. Geophys. Res.*, *102*, 3761–3778, 1997.

Feichter, J., E. Kjellström, H. Rodhe, F. Dentener, J. Lelieveld, and G.-J. Roelofs, Simulation of the tropospheric sulfur cycle in a global climate model, *Atmos. Environ.*, *30*, 1693–1707, 1996.

Feichter, J., U. Lohmann, and I. Schult, The atmospheric sulfur cycle and its impact on the shortwave radiation, *Clim. Dyn.*, *13*, 235—256, 1997.

Graf, H.-F., J. Feichter, and B. Langmann, Volcanic sulfur emissions: Estimates of source strength and its contribution to the global sulfate distribution, *J. Geophys. Res.*, *102*, 10,727—10,738, 1997.

Hartley, D., D. Williamson, P. Rasch, and R. Prinn, Examination of tracer transport in the NCAR CCM2 by comparison of $CFCl_3$ simulations with ALE/GAGE observations, *J. Geophys. Res.*, *99*, 12,855–12,896, 1994.

Kasibhatla, P., W. L. Chameides, and J. St. John, A three-dimensional global model investigation of seasonal variations in the atmospheric burden of anthropogenic sulfate aerosols, *J. Geophys. Res.*, *102*, 3737–3760, 1997.

Kent, G. S., M. P. McCormick, and P.-H. Wang, Validation of Stratospheric Aerosol and Gas Experiments i and ii satellite aerosol optical depth measurements using surface radiometer data, *J. Geophys. Res.*, *99*, 10,333—10,339, 1994.

Kiehl, J. T., T. L. Schneider, P. J. Rasch, M. Barth, and J. Wong, Radiative forcing due to sulfate aerosols from simulations with the National Center for Atmospheric Research Community Climate Model, Version 3, *J. Geophys. Res.*, inpress, 1999.

Kiehl, J. T., J. Hack, G. B. Bonan, B. A. Boville, B. P. Briegleb, D. L. Williamson, and P. J. Rasch, *Description of the NCAR Community Climate Model (CCM3)*, NCAR Tech. Note, NCAR/TN-420+STR, Nat. Cent. for Atmos. Res., Boulder, Colo., 1996.

Langner, J., and H. Rodhe, A global three-dimensional model of the tropospheric sulfur cycle, *J. Atmos. Chem.*, *13*, 225—263, 1991.

Langner, J., H. Rodhe, P. J. Crutzen, and P. Zimmermann, Anthropegenic influence on the distribution of tropospheric sulphate aerosol, *Nature*, *359*, 712—715, 1992.

Lelieveld, J., G.-J. Roelofs, L. Ganzeveld, J. Feichter, and H. Rodhe, Terrestrial sources and distribution of atmospheric sulphur, *Phil. Trans. R. Soc. Lond.*, *352*, 149–158, 1997.

Müller, J.-F., and G. P. Brasseur, IMAGES: A three-dimensional chemical transport model of the global troposphere, *J. Geophys. Res.*, *100*, 16,445—16,490, 1995.

Pham, M., J.-F. Müller, G. Brasseur, C. Granier, and G. Megie, A three-dimensional study of the tropospheric sulfur cycle, *J. Geophys. Res.*, *100*, 26,061—26,092, 1995.

Randall, D. A. (Ed.), Special issue devoted to the Climate Systems Model, *J. Clim.*, *11*, 383 pp, 1998.

Rasch, P. J., and J. E. Kristjánsson, A comparison of the CCM3 model climate using diagnosed and predicted condensate parameterizations., *J. Clim.*, *11*, 1587—1614, 1998.

Roelofs, G.-J., J. Lelieveld, and L. Ganzeveld, Simulation of global sulfate distribution and the influence on effective cloud drop radii with a coupled photochemistry-sulfur cycle model, *Tellus, Ser. B*, *50*, 224–242, 1998.

Turco, R. P., R. C. Whitten, and O. B. Toon, Stratospheric aerosols: obvservations and theory, *Revs. Geophys. Space Phys.*, *20*, 233—279, 1982.

Twomey, S. A., Pollution and the planetary albedo, *Atmos. Environ.*, *8*, 1251–1256, 1974.

Waugh, D. W., et al., Three-dimensional simulations of long-lived tracers using winds from MACCM2, *J. Geophys. Res.*, *102*, 21,493–21,513, 1997.

Wojcik, G. S., and J. S. Chang, A re-evaluation of sulfur budgets, lifetimes and scavenging ratios for Eastern North America, *J. Atmos. Chem.*, *26*, 109—145, 1997.

M. C. Barth, J. T. Kiehl, and P. J. Rasch, NCAR, P. O. Box 3000, Boulder, CO 80307. (email: pjr@ucar.edu)

C. M. Benkovitz and S. E. Schwartz, Brookhaven National Laboratory, Upton, NY 11973.

(Received December 21, 1998; revised July 16, 1999; accepted July 21, 1999.)